Analysis and Design of a Novel Mini-platform Employing Vibration Micro-motors[*]

Panagiotis Vartholomeos and Evangelos Papadopoulos

Department of Mechanical Engineering, National Technical University of Athens, 15780 Athens, Greece
barthol@central.ntua.gr , egpapado@central.ntua.gr

Abstract . – **This paper presents the analysis and design of a novel mini-robotic platform that is able to perform translational and rotational sliding with sub-micrometer positioning accuracy and develop velocities up to 1.5** ***mm/s.*** **The platform actuation system employs vibration micro-motors. The dynamic model of the platform and of its actuation system is presented, and analytical expressions are derived which provide design guidelines for the platform. Simulations are performed which verify the analytical results and demonstrate the platform capabilities. The platform design is simple, compact and of low cost. Also the energy supply of the mechanism can be accomplished in an untethered mode using simple means such as single cell batteries.**

Index terms – micro-positioning, vibration motors, dynamic simulation

I. INTRODUCTION

In the last decade, micro-robotics has become an increasingly important field of research. Domains of application such as micro fabrication, biotechnology, microscopy and opto-electronics demand miniaturized or micro-robotic platforms that provide ultra high precision, flexibility and a wide mobility range. Extensive research has been carried out in the design and realization of miniature mobile robotic platforms. Motion principles and actuation mechanisms that combine sub-micrometer motion of high resolution and the speed virtues of coarse positioning have been the subject of intensive studies, see for example [1], [2].

A lot of work has been carried out especially in piezoelectric micro-positioning systems, for example see [1-5]. Possibly the most popular micro-positioning motion mechanism is the stick-slip principle which is implemented using piezoelectric actuators. A characteristic example is the micro-platform presented in [1] which is capable of positioning accuracy of less than $200nm$ and provides velocities of up to $5mm/s$. A different motion principle based on piezo-actuators and electromagnets, is presented in [5], where the interaction of piezo-electric elements and electromagnetic actuators results in a step length of $7.0\mu m$ and a velocity of $1.16mm/s$.

Although piezoelectric actuators provide the required positioning resolution and actuation response for micro-positioning, usually they suffer from complex power units that are expensive and cumbersome and which do not allow for untethered operation. Furthermore, piezoelectric actuators are complex systems that exhibit non-linear behavior and as a result they lack accurate mathematical model that can provide a reliable prediction of the system's behavior.

This paper presents the analysis and design of a novel, simple and compact mini-robotic platform that is able to perform translational and rotational sliding with sub-micrometer positioning accuracy and velocities up to $1.5mm/s$. All the components of the mechanism including its driving units are of low cost and readily available. The motion mechanism is based on the interaction of centripetal forces due to vibration of micro-motors and friction forces at the base supports. The concept was inspired by observing the motion of devices that vibrate, such as cellular phones or unbalanced washing machines [6, 7]. First, analysis of the motion principle physics is provided. Then, the dynamic model of the platform and of its actuation system is presented and analytical expressions are derived which provide guidelines for the design of the platform. Using a basic platform design, simulations are performed which verify the analytical results and demonstrate the platform capabilities. Finally, a set of equations for open loop control of the platform are derived and tested through a simple example.

II. MOTION PRINCIPLE

The motion principle is first demonstrated, using a simplified single DOF mobile platform of mass M. The motion mechanism uses a mass m rotated by a motor O mounted on the platform as shown in Fig 1.
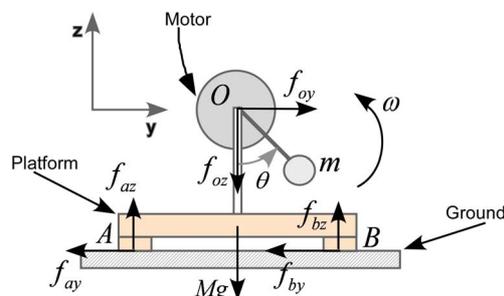
Fig. 1. Simplified 1 DOF platform.

Assume that the mass m rotates on a vertical plane at a constant speed ω, about point O and that the platform is

constrained to move along the y-axis only. The forces exerted on point O due to the rotating mass m are given by (moment due to the rotating mass is considered negligible):

$$f_{oy} = mr\omega^2 \sin\theta$$
$$f_{oz} = -mg - mr\omega^2 \cos\theta \quad (1)$$

where g is the acceleration of gravity, and r is the length of the link between m and O. If the rotational speed ω is above a critical value, then f_{oy} overcomes static friction forces and the platform begins to slide. The equations describing the motion along the y-axis and the static equilibrium along the z-axis are:

$$M\ddot{y} = f_{oy} - \mu(f_{az} + f_{bz})$$
$$f_{az} + f_{bz} - Mg + f_{oz} = 0 \quad (2)$$

where μ is the coefficient of kinetic friction. The results of a numerical simulation of the above equations are presented in Fig 2.
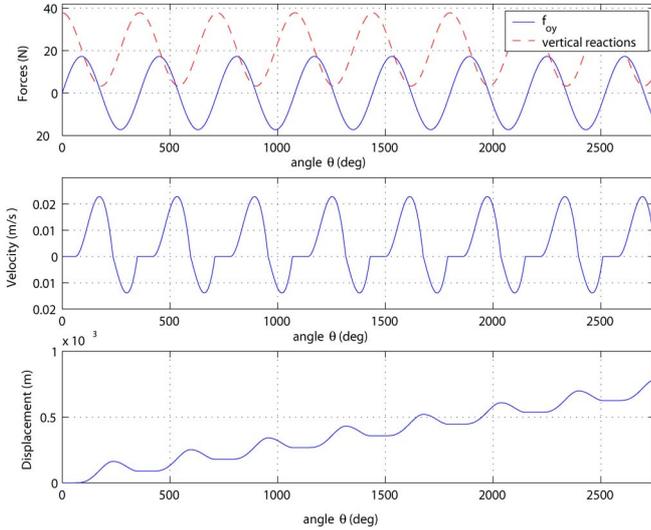
Fig. 2. Forces and displacement of a 1DOF mechanism.

From the third plot of Fig. 2, it becomes apparent that the platform exhibits a net displacement towards the positive y direction. This is due to the fact that the vertical reactions exerted on the platform by the ground, lead by $90°$ the lateral force f_{oy}, see first plot of Fig 2. As a result, during the second quadrant of the rotation of mass m, where most of the forward motion takes place, the vertical reaction reduces from the value $(M+m)g$ to its minimum value. On the contrary during the fourth quadrant, where most of the reverse sliding takes place, the vertical reaction increases from $(M+m)g$ to its maximum value. Hence, during reverse sliding the friction forces are greater than the friction forces during forward sliding and the velocities developed during reverse motion are smaller, see plot 2, Fig. 2. Consequently, the reverse displacement is smaller compared to the forward displacement, resulting to a net forward displacement of the platform to the left. Reversal of ω will lead to a reversal of the direction of motion.

III. 3DOF PLATFORM

The design of a 3DOF mini-robotic platform takes advantage of the aforementioned motion principle and focuses towards the creation of a mobile mini-robot with the following design objectives: The platform should be capable of performing x, y, θ motion. It should be able to reach positioning resolution of the order of sub-microns and also it should be able to develop speeds of several mm/s. Its size should be less than 5 cm^2 so that multi-robot cooperation within a workspace of limited area would be feasible. Finally the cost of constructing and powering the robotic platform should be as small as possible.

Platform base: The geometry of the base of the mini-robot is an equilateral triangle of length l. Three small rigid supports A, B and C located at each vertex of the triangle provide the contact points between the platform and the ground, see Fig. 3a. The 3-contact point configuration is favored due to the fact that it is not over-constrained and ensures static equilibrium along the vertical axis. The center of mass of the base coincides with the geometrical center of the equilateral triangle.
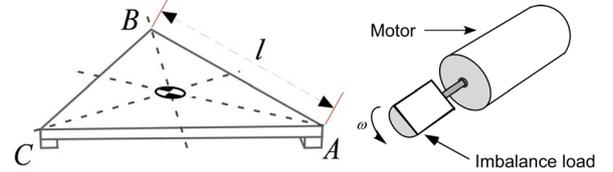
Fig. 3. (a) Platform base. (b) Vibrating motor.

Actuators: The actuation of the platform employs miniature-vibrating motors. The vibrating motor is axially coupled to an imbalance load see Fig. 3b, and the control input is the spin speed ω of the motor. During rotation, the eccentric mass of the load generates dynamic forces, which are applied to the platform.

Three identical vibrating motors D, E and F, are symmetrically mounted on top of the platform as shown in Fig. 4.
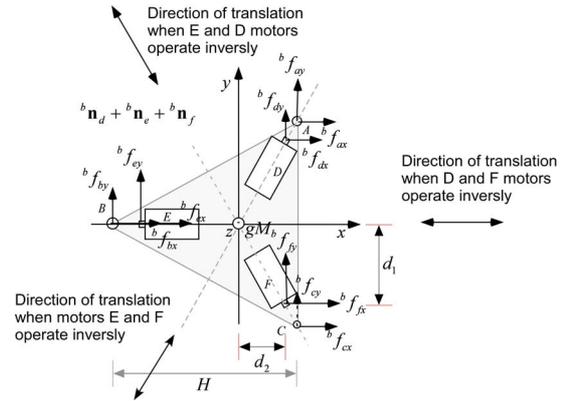
Fig. 4. Actuation and reaction forces.

If actuators D and F spin at an opposite sense of rotation while E is inactive, then the platform slides along the positive x-axis, if their sense of rotation is reversed then sliding occurs along the negative x-axis. Similarly when D and E or E and F actuators spin at an opposite

sense of rotation, then the platform slides at a direction angle of 120° or 240° with respect to the x-axis respectively, see Fig 4. When all actuators spin with same sense of rotation, then pure rotation about the platform center of mass (CM) is performed.

IV. DYNAMICS

1. Dynamic model

The assumptions on which the dynamic model is based are: (i) The imbalance load can be modeled as a point mass m, rotating at a distance r from the motor axis. (ii) All actuators are identical. (iii) Every rotating mass m spins at a constant speed ω and the plane of rotation is normal to the plane of the base. (iv) All rotating masses are in phase. (v) The Coulomb friction model with constant friction coefficient μ is adopted. (vi) All involved bodies are rigid. (vii) Due to platform symmetry, it is assumed that actuation forces along the base plane and moments about the z-axis are equally distributed on the three supports.

The platform analysis involves the body-fixed frame B and the inertial frame O. The adopted notation is ${}^i f_j$ where the superscript i is the frame index and subscript j is the component x, y, z index. The b superscript denotes frame B. Frame O uses no superscript. Forces ${}^b\mathbf{f}_a, {}^b\mathbf{f}_b, {}^b\mathbf{f}_c$ include the normal and frictional contact forces at contact points A, B and C respectively. The angle θ is the angle of the eccentric mass with respect to the vertical axis as shown in Fig. 5. Forces ${}^b\mathbf{f}_d, {}^b\mathbf{f}_e, {}^b\mathbf{f}_f$ and ${}^b\mathbf{n}_d, {}^b\mathbf{n}_e, {}^b\mathbf{n}_f$ (see Fig. 4), are the actuation forces and moments exerted on and about the corresponding motors and are given by:

$$
\begin{aligned}
{}^b f_{ix} &= -mr\omega^2 \sin\phi_i \sin\theta \\
{}^b f_{iy} &= mr\omega^2 \cos\phi_i \sin\theta \\
{}^b f_{iz} &= -mg - mr\omega^2 \cos\theta \\
{}^b n_{ix} &= -mgr\cos\phi_i \sin\theta, \; {}^b n_{iy} = -mgr\sin\phi_i \sin\theta \\
i &= \{d, e, f\}, \; \phi_i = \{60°, 180°, -60°\},
\end{aligned}
\tag{3}
$$

where $\omega = \dot\theta$ is motor angular velocity and r is the imbalance mass m distance from the axis of rotation. The position vector describing the contact points A, B and C are denoted by ${}^b r_a, {}^b r_b, {}^b r_c$ and the position vectors describing the tip of the motors axis D, E and F are denoted by ${}^b r_d, {}^b r_e, {}^b r_f$. The Newton-Euler equations of the platform are [8]:

$$
M\ddot{\mathbf{x}} = \mathbf{R} \sum_i ({}^b\mathbf{f}_i) \quad i = \{a, b, c, d, e, f\}
\tag{4}
$$

$$
{}^b\mathbf{I}\dot{\boldsymbol{\omega}} + {}^b\boldsymbol{\omega} \times {}^b\mathbf{I}\,{}^b\boldsymbol{\omega} = \sum_i ({}^b\mathbf{r}_i \times {}^b\mathbf{f}_i) + \sum_j {}^b\mathbf{n}_j
$$
$$
i = \{a, b, c, d, e, f\}, \; j = \{d, e, f\}
\tag{5}
$$

where $\mathbf{R}$ is the rotation matrix between frames B and O, $\boldsymbol{\omega}$ is the base angular velocity, ${}^b\mathbf{I}$ is the platform inertia matrix and $\mathbf{x} = [x, y]^T$ is the base CM position in the inertial frame. Due to the platform symmetry and planar motion, $\boldsymbol{\omega} = [0, 0, \dot\psi]^T$, $\mathbf{I}$ is substituted by I_{zz} and the term ${}^b\boldsymbol{\omega} \times {}^b\mathbf{I}\,{}^b\boldsymbol{\omega}$ is zero.

2. Threshold values of spin speed ω

The platform is not able to slide for all values of motor angular velocities ω. In particular if ω is below a critical value ω_{sl}, then actuation forces are not large enough to induce motion. If speed ω is greater than the critical value ω_{sl}, then forces are strong enough to counteract friction and consequently to induce motion. On the other hand, if ω is very large i.e. greater than a critical value ω_{tip}, then tipping occurs and platforms stability is lost. The range of permissible driving speeds $\omega \in \left[\omega_{sl}, \omega_{tip} \right]$ is defined as the operating range of the platform. The objective is to choose parameter values in order to maximize the displacement per step and to maximize the value of ω_{tip} so that platform velocity is maximized. To this aim, analytical expressions are derived which relate the minimum ω_{sl} and minimum ω_{tip} to platform's physical parameters. Also, the analytical expression for the total displacement per cycle is derived and its relation to the design parameters is examined. Fig. 5 depicts the circular trajectory described by each rotating mass during a complete cycle, and also relates the motion state of the platform to the angular position of the spinning mass. It is assumed that $\omega > \omega_{sl}$ i.e. that sliding is induced.
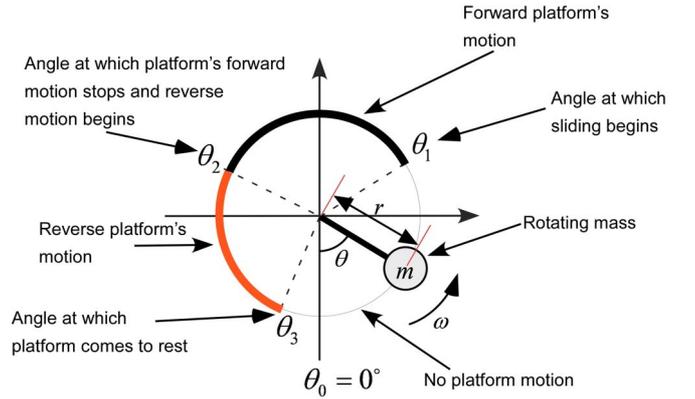
Fig. 5. Mass rotation during a single cycle.

For simplification purposes, and for exploiting the merits of analytical solutions, ω_{sl} and ω_{tip} are determined only for the cases of pure translation and pure rotation. Consider the case of pure translation along the x-axis where $\omega = \omega_{sl}$, sliding is impending and friction forces have reached the static limit:

$$
{}^b f_{ax} + {}^b f_{bx} + {}^b f_{cx} = \mu({}^b f_{az} + {}^b f_{bz} + {}^b f_{cz})
\tag{6}
$$

Solving (6) for ω, yields:

$$
\omega_{sl} = \left(\frac{\mu\, g(M + 3m)}{mr(\sqrt{3}\sin\theta - 2\mu\cos\theta)} \right)^{1/2}
\tag{7}
$$

Where μ is the coefficient of friction and parameters M, m and r are defined in Fig. 4 and 5. From (7), it is evident that for every θ there is a particular critical speed ω_{sl}. Since the mass describes complete circles, it is necessary to determine the angle θ at which the minimum ω_{sl} occurs. Differentiating (7) with respect to angle θ and setting the result equal to zero yields the angle at which the minimum ω_{sl} occurs:

$$\theta_{\omega sl\min} = \tan^{-1}(-\frac{\sqrt{3}}{2\mu}) \qquad (8)$$

Substituting (8) into (7) and after simple algebraic manipulations, the minimum critical speed for translation is obtained:

$$\omega_{sl\min} = \left(\frac{(\frac{2\mu}{\sqrt{3}})g(3m+M)}{2mr(\sqrt{1+(\frac{2\mu}{\sqrt{3}})^2})} \right)^{1/2} \qquad (9)$$

It may happen that due to system geometry, the platform reaches a tipping condition before slip. In this case, the equilibrium of moments about the y-axis is marginally stable and reactions ${}^b f_{az}$ and ${}^b f_{cz}$ are reduced to zero. Taking moments about contact point B and solving for ω_{tip} yields:

$$\omega_{tip} = \left(\frac{-g\,H\,(3\,m\,+\,M)}{m\,r\,(2\cos\theta(H+3\,d_2)+3\sqrt{3}\sin\theta h_o)} \right)^{1/2} \quad (10)$$

where parameter H is the height of the triangular base as shown in Fig. 4 and parameter h_o is the distance from the motor axes to the ground.

$$\theta_{tip\min} = \tan^{-1}(\frac{3\sqrt{3}h_o}{2(\text{H}+3d_2)}) \qquad (11)$$

Substituting (11) into (10), and writing $d_2 = aH$, where $a \in [0,1/3]$ is a constant of proportionality, results to:

$$\omega_{tip\min} = \left(\frac{(1+3a)^{-1}2H(1+3a)g(3m+M)}{2mr((3\sqrt{3}h_o)^2+(2H(1+3a))^2)^{1/2}} \right)^{1/2} \quad (12)$$

The condition for $\omega_{sl\min} < \omega_{tip\min}$ yields:

$$(\frac{\sqrt{3}}{2\mu})^2 + 1 \geq (\frac{3\sqrt{3}h_o}{2H})^2 + (1+3a)^2 \qquad (13)$$

Equation (13) is a design condition, which must be met to ensure slip during linear motion. Next, the case of pure rotation is studied.

In order to induce pure rotation about the CM of the platform all three masses are rotating at the same speed, in a clockwise or anticlockwise direction depending on the desired sense of rotation. Following similar reasoning with the translational case it is found that:

$$\omega_{sl} = \left(\frac{2g(3+M/m)}{3r(4+a^2\mu^{-2})^{1/2}} \right)^{1/2}, \quad \omega_{tip} = (\frac{g(3+M/m)}{3r})^{1/2} \, (14)$$

Equations (14) are design equations that contribute to the determination of parameters μ, r, m and M.

3. Analytical derivation of the displacement

The net displacement per cycle is found as follows. A single motion step of the platform is broken up into the forward phase (forward displacement) and the reverse phase (reverse displacement), see Fig. 5. Starting from the forward phase, the slip angle θ_1 is derived from (7):

$$\theta_1 = f^{-1}(\omega) \qquad (15)$$

Then, the linear acceleration of the forward phase is integrated with respect to θ and yields (all motion variables are expressed with respect to frame O):

$$v_{forward}(\theta') = \frac{1}{M\omega} \int_{\theta 1}^{\theta'} (\ddot{x}_{forward})d\theta \qquad (16)$$

Where $x_{forward}$ is the displacement along the direction of motion. Next, $v_{forward}(\theta') = 0$ is solved for θ'. Then setting $\theta_2 = \theta'$ and integrating v from θ_1 to θ_2 yields:

$$x_{forward} = \frac{1}{M\omega^2} \int_{\theta 1}^{\theta 2} v_{forward}(\theta')d\theta' \qquad (17)$$

At an angle θ_2 the forward phase stops and the reverse phase begins. Repeating the previous steps for the reverse phase, yields:

$$v_{reverse}(\theta'') = \frac{1}{M\omega} \int_{\theta 2}^{\theta''} a\,d\theta \qquad (18)$$

$$x_{reverse} = \frac{1}{M\omega^2} \int_{\theta 2}^{\theta 3} v_x(\theta'')d\theta'' \qquad (19)$$

The net displacement is a function of ω and is given by:

$$x_{total} = x_{forward} + x_{reverse} \Rightarrow$$
$$x_{total} = \frac{1}{2M\omega^2}(-\mu g(3m+M)(\theta_1-\theta_3)(\theta_1-$$
$$2\theta_2+\theta_3)+2mr\omega^2(-2\mu(\cos\theta_1-2\cos\theta_2+$$
$$\cos\theta_3+(\theta_1-\theta_2)\sin\theta_1-(\theta_2-\theta_3)\sin\theta_2)+ \qquad (20)$$
$$\sqrt{3}((-\theta_1+\theta_2)\cos\theta_1-(\theta_2-\theta_3)\cos\theta_2$$
$$+\sin\theta_1-\sin\theta_3))$$

Similarly, the net rotational motion is given by:

$$\psi_{total} = \frac{1}{3I\omega^2}(\mu H(-g(3m+M)(\theta_1-\theta_3)(\theta_1-$$
$$2\theta_2+\theta_3)-6mr\omega^2(\cos\theta_1-2\cos\theta_2+\cos\theta_3+$$
$$(\theta_1-\theta_2)\sin\theta_1-(\theta_2-\theta_3)\sin\theta_2))- \qquad (21)$$
$$3mr\omega^2((\theta_1-\theta_2)\cos\theta_1+(\theta_2-\theta_3)\cos\theta_2-$$
$$\sin\theta_1+\sin\theta_3)(\sqrt{3}d_1+3d_2))$$

4. Design parameters

The equations derived above provide the following design guidelines: From (13) and (14) it is clear that in order to increase ω_{tip}, parameter H or equivalently the base surface should be maximized and parameter h_o, i.e. the motor height, should be minimized. The material at the contact points should exhibit a low coefficient of friction in order to increase the total displacement per step as indicated by (20) and (21). The parameter r according to

(20) and (21) is proportional to the total displacement per cycle, but according to (12) and (14) ω_{tip} is inversely proportional to the square root of r. An average value of r is selected in order to increase the step length per cycle with out reducing substantially the value of ω_{tip}.

The above design rules apply to both translational and rotational motion and it is evident that they are extended to the general plane motion. On the other hand, increasing the value of parameter a decreases ω_{tip} translational but increases the value of ω_{tip} rotational. Hence, an average value of parameter a is desired in order to balance between translational and rotational operating range. It should be mentioned that the limited workspace of the working environment does not allow for a platform with side length larger than $5cm$ and consequently this imposes an upper limit to parameter H. Finally from (20) and (21) it is observed that mass M and inertia I should be kept low, otherwise the net displacement is reduced considerably.

A typical vibrating micro-motor that complies with the above guidelines and the dimensional constraints of the platform is the SHICOH SE-S4E (B1A) coreless vibration motor whose mechanical and electrical characteristics are depicted in Table 1. The consideration of the above analysis leads to the set of design parameter values listed on Table 2.

TABLE 1
VIBRATING MOTOR SE-S4E SPECIFICATIONS

Parameter	Value	Parameter	Value
Rated Voltage	1.3V	Vibration	$12.74 m/s^2$
Operating Voltage	0.9V~1.6V	Weight of motor	1.1g
Road Speed	9000min⁻¹	Radius of unbalanced mass	2mm
Starting Voltage	0.8V	Motor diameter	4mm
Starting Current	120mA	Motor length	14.4 mm
Armature Resistance	12 Ω		

TABLE 2
DESIGN PARAMETERS

Parameter	Value	Parameter	Value
r	0.002-0.004 m	l	0.05m
m	0.001kg	h_o	0.004m
M	0.03 kg	μ	0.5

V. SIMULATION

A dynamic simulation of the generalized plane motion of the platform is implemented using MATLAB and SIMULINK. The aim of the simulation, is to verify analytical results and to demonstrate the platform motion capabilities.

1. *Software design.* Simulation software comprises: (i) A complete dynamic model of the platform (ii) A dynamic model of the actuators (iii) A set of functions that solve for the reaction forces and friction forces at each contact point. (iv) A differential kinematics model. At every time step the procedure presented in Fig. 6 is implemented. The input to the system is either the motors speed or the motors input voltage.
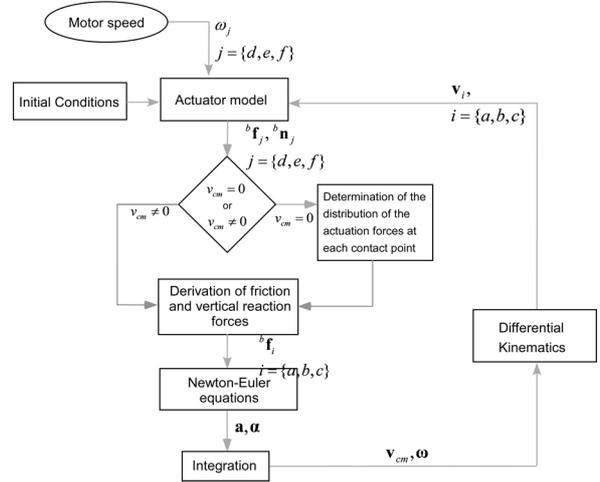
Fig. 6. Program flow chart.

2. *Simulation example.* The simulation example demonstrates pure translation at a direction 120° with respect to the x-axis. To this aim rotational speeds of motors D and E are set at $\omega_d = 2250rpm$ and $\omega_e = -2250rpm$ respectively. Plot 1 of Fig. 7 demonstrates the platform displacement along the x and y axis as a function of time. Plot 2 demonstrates the velocities along the x and y-axis and Plot 3 depicts the lateral actuation forces, the friction forces, the variation of static friction limit (Coulomb level) and the centre of mass velocity for a single cycle. Observe that when the actuation forces exceed the static friction limit, the friction is saturated at that limit and motion is induced. The net displacement per cycle for $\omega_d = 2250rpm$ is $4\mu m$. The average velocity is $0.15 \cdot 10^{-3} m/s$.
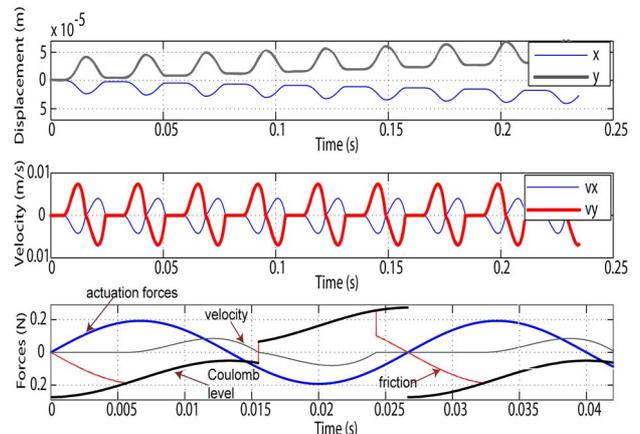
Fig .7. Translational motion with $\omega_d = 2250rpm$ and $\omega_e = -2250rpm$.

It should be noted that the motion principle holds even

for phase differences up to $15°$. On the contrary, the synchronization assumption (same spin speed) has to be strictly satisfied or otherwise the phase difference will increase by $(\omega_e - \omega_d)t$ leading to an unpredictable platform behavior. Hence, closed loop control of the motors rotational speed, or utilization of stepper motors instead of DC motors, is essential for reliable operation.

VI. OPEN LOOP CONTROL

It is important to derive an open loop control of the platform in order to be in position to specify the required ω (control input) that results to the desired displacement per cycle (input command). To this aim, the inverse function $\omega = f^{-1}(x_{total})$ is calculated numerically, where ω is the motor angular speed and x_{total} is the net displacement during a cycle. The determination of the inverse function requires the solution of a non-linear system of four equations which is formed by (7), $v_{forward}(\theta_2) = 0$, $v_{reverse}(\theta_3) = 0$ and (20) expressed in the following functional form:

$$\begin{aligned}
f_1(\theta_1, \omega) &= 0, \\
f_2(\theta_1, \theta_2, \omega) &= 0, \\
f_3(\theta_2, \theta_3, \omega) &= 0, \\
f_4(\theta_1, \theta_2, \theta_3, \omega) &= 0
\end{aligned} \qquad (22)$$

Given the desired x_{total}, the system is numerically solved for ω. Following the same reasoning, a set of similar equations is generated for the rotational motion.

As an example of the open loop control efficacy, consider the case where it is desired to perform the following path: (i) $25\mu m$ translation along the positive x-axis implemented through five steps of $5\mu m$, (ii) $1mrad$ anticlockwise rotation about z, implemented in 5 steps of $0.2mrad$, (iii) again, perform a $25\mu m$ translation at an angle of $1mrad$ with respect to the x-axis. Solving (22), it is found that $x = 5\mu m$ requires $\omega_{trans} = 2256rpm$. Similarly, it is found that the rotational step of $0.2mrad$ requires $\omega_{rot} = 2196rpm$. The time duration of each control command is set to: $t_{control} = (Number\ of\ steps)60/\omega$.
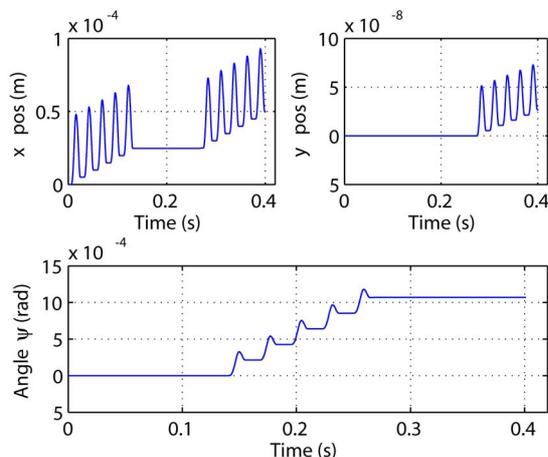
Fig. 8. *x, y* and *ψ* displacement.

Plot 1 of Fig. 8 demonstrates the trajectory of the platform along the x-axis. Plot 2 depicts the trajectory along the y-axis and Plot 3 demonstrates the trajectory of the angle ψ. The step sizes are the expected ones.

Inertia of the spinning mass was neglected in this example. In a hardware experiment however, inertia will be present and during large acceleration or deceleration will affect the platform motion by generating transient motion and thus reducing the platform resolution to a few steps.

VII. CONCLUSIONS

The paper presented the analysis and design of a novel mini-robotic platform that is able to perform translational and rotational motion on the plane. The mini-robot can be constructed from inexpensive and readily available components, and its power requirements can be provided by a single cell battery. Analytical expressions and simulation results predict that the positioning resolution of the platform is of sub-micrometer order, its maximum step is about $40\mu m$ and its maximum average velocity is about $1.5mm/s$.

REFERENCES

[1] Breguet Jean-Marc, Clavel Reymond, "Stick and Slip Actuators: design, control, performances and applications," *International Symposium on Micromechatronics and Human Science (MHS)*, (Nagoya), pp.89-95, 1998.

[2] Zesch Wolfgang, Buchi Roland, Codourey Alain, Siegwart Roland, "Inertial Drives for Micro- and Nanorobots: An analytical study," *SPIE Conf. on Microrobots and Micromechanical System*s, Oct 1995, Philadelphia.

[3] Schmoeckel F., Fatikow S, "Smart Flexible Microrobots for Scanning Electron Microscope (SEM) Applications," *SPIE's 7th Int. Symp. On Smart Structures and Materials: Integrated systems*, Newport Beach, California, USA, 5-9 March 2000.

[4] Martel Sylvain et al., "THREE-LEGGED WIRELESS MINIATURE ROBOTS FOR MASS-SCALE OPERATIONS AT THE SUB-ATOMIC SCALE," *Proceedings of the 2001 IEEE International Conference on Robotics & Automation*, Seoul, Korea, May 21-26, 2001.

[5] Aoyama Hisayuki, Fuchiwaki. Ohmi, "Flexible Micro-Processing by Multiple Micro Robots in Sem," *Proceedings of the 2001 IEEE International Conference on Robotics & Automation*, Seoul, Korea, May 21-26, 2001.

[6] Papadopoulos E., Papadimitriou I., "Modelling, Design and Control of a Portable Washing Machine during the Spinning Cycle," *IEEE/ASMEInternational Conference on Advanced Intelligent Mechatronics System (AIM 2001), 8-11 July 2001,* Como Italy, pp. 899-904.

[7] Badami, V.V. and Chibat, N.W., "Home Appliances Get Smart," IEEE Spectrum v. 35 n 8, August 1998, pp. 36-43

[8] L.Sciavicco and B. Siciliano, *Modelling and Control of Robot Manipulators*, Springer-Verlag London Ltd, 2001.